Simultaneous Measurement of Three-dimensional Joint Kinematics and Ligament Strains with Optical Methods

Trevor J. Lujan, Spencer P. Lake, Timothy A. Plaizier,
Benjamin J. Ellis, Jeffrey A. Weiss

Department of Bioengineering
University of Utah
Salt Lake City, UT

In Press, *Journal of Biomechanical Engineering*
August 31, 2004

Keywords: strain measurement, kinematics, ligament, optical methods, accuracy, precision

Corresponding Author:

Jeffrey A. Weiss, Ph.D.
Department of Bioengineering
University of Utah
50 South Central Campus Drive, Room 2480
Salt Lake City, Utah 84112-9202
801-587-7833
jeff.weiss@utah.edu

ABSTRACT

The objective of this study was to assess the precision and accuracy of a non-proprietary, optical three-dimensional (3D) motion analysis system for the simultaneous measurement of soft tissue strains and joint kinematics. The system consisted of two high-resolution digital cameras and software for calculating the 3D coordinates of contrast markers. System precision was assessed by examining the variation in the coordinates of static markers over time. 3D strain measurement accuracy was assessed by moving contrast markers fixed distances in the field of view and calculating the error in predicted strain. 3D accuracy for kinematic measurements was assessed by simulating the measurements that are required for recording joint kinematics. The field of view (190 mm) was chosen to allow simultaneous recording of markers for soft tissue strain measurement and knee joint kinematics. Average system precision was between ±0.004 mm and ±0.035 mm, depending on marker size and camera angle. Absolute error in strain measurement varied from a minimum of ±0.025% to a maximum of ±0.142%, depending on the angle between cameras and the direction of strain with respect to the camera axes. Kinematic accuracy for translations was between ±0.008 and ±0.034 mm, while rotational accuracy was ±0.082 to ±0.160 degrees. These results demonstrate that simultaneous measurement of 3D soft tissue strain and 3D joint kinematics can be performed while achieving excellent accuracy for both sets of measurements.

INTRODUCTION

The measurement of strain is of fundamental interest in the study of soft tissue mechanics. In studies of musculoskeletal joint mechanics, the accurate measurement of three-dimensional joint kinematics is equally important. By simultaneously quantifying the strains in soft tissues such as ligaments and the joint kinematics in response to externally applied loads, it is possible to elucidate the role of these structures in guiding and restraining joint motion and to identify potential injury methods and clinical treatments [1-3]. Further, simultaneous acquisition of joint kinematics and strain fields can be used to drive and validate subject-specific models of ligament and joint mechanics [4].

The simultaneous measurement of joint kinematics and soft tissue strain is typically accomplished by using a combination of two or more different technologies. Joint kinematics are commonly quantified using video-based techniques [5,6], instrumented spatial linkages (ISLs) [7,8] or electromagnetic tracking systems [9-11]. ISL systems require the attachment of a bulky mechanical linkage across the joint, while electromagnetic tracking systems are often plagued by interference from ferrous materials, limiting their applicability. In contrast, there are relatively few techniques that are capable of measurement of three-dimensional soft tissue strains. Alternatives include the use of one-dimensional measurements from contact devices such as DVRTs [12,13]. Optical methods are currently considered to be the best option for 3D strain measurement on visible soft tissues. These methods use the direct linear transformation to calculate 3D strain measurements from two or more cameras [4,14]. Previous optical systems were primarily based on super VHS video, yielding an effective vertical resolution of 400 lines. This limited resolution requires the use of extremely small fields of view to achieve accuracies of ±0.1-0.5% error in percent strain [14]. This precludes the simultaneous tracking of markers for kinematic measurements, since a larger field of view is needed to see both the strain and kinematic markers. Currently available systems based on digital cameras typically use vendor-supplied proprietary cameras and/or framegrabbers. These systems primarily use digital cameras that have much better resolution and sensitivity than video-based systems. However, the use of proprietary vendor-supplied hardware is often costly and ties the support and upgrade of the system to a particular vendor or system integrator.

Due to ongoing improvements in the sensitivity and resolution of charge-coupled devices (CCDs), modern progressive-scan digital cameras can provide images with very high quality and resolution. The improved spatial resolution (typically at least 1024x1024) opens up the possibility of using a field of view that is large enough to track markers for both soft tissue strain and joint kinematics. The use of cameras and framegrabbers from individual vendors is especially attractive since it eliminates the need for proprietary, vendor-specific hardware and software. The objective of this study was to develop a methodology for simultaneous measurement of three-dimensional (3D) soft tissue strain and joint kinematics using a non-proprietary digital camera system, and to quantify the errors associated with these measurements in a test setup that mimicked the study of knee ligament biomechanics.

MATERIALS AND METHODS

Measurement System. The measurement system consisted of two high-resolution digital cameras (Pulnix TM-1040, 1024x1024x30 frames per second (fps), Sunnyvale, CA) equipped with 50 mm 1:1.8 lenses and extension tubes, two frame grabbers (Bitflow, Woburn, MA) and Digital Motion Analysis Software (DMAS, Spica Technology Corporation, Maui, HI). The cameras were configured to record 6 fps directly to computer memory, requiring 2.1 MB of memory per frame. The cameras were focused at a target with a 190 mm diagonal field of view (FOV). The DMAS software tracked marker centroids in both camera views automatically and applied the modified direct linear transformation (DLT) to calculate the 3D centroid coordinates [15]. Preliminary tests demonstrated that black markers against a white background provided superior contrast and therefore system accuracy in comparison to markers covered with reflective tape, while two 100 W incandescent lights provided better contrast than halogen or fluorescent lighting. In the following sections, all instrument accuracy values are per the manufacturer.

A 3D calibration frame was manufactured. Twenty-seven white Delrin spherical markers (4.75 mm dia.) were arranged in three horizontal planes, with a 3x3 grid pattern on each plane and 60 mm marker spacing. The exact coordinates of each marker centroid were determined with a coordinate measuring machine (Zeiss Eclipse 4040, accuracy ±0.0004 mm). These coordinates were used for DLT calibration.

Precision. The precision was determined by examining the variation of the 3D positions of stationary markers over time. After calibration, two different frames with twelve 4.75 and 2.38 mm dia. spherical markers were recorded for 25 seconds. The dimensions of these markers were chosen to be the exact same size as the kinematic markers (4.75 mm dia) and the strain markers (2.38 mm dia) used during actual biomechanical testing in our laboratory. The variation in marker position was determined by computing two standard deviations of the length of their position vector and the individual x, y and z coordinates over time. Experiments were repeated at camera angles of 30, 60 and 90 degrees (Figure 1). To evaluate the precision of the system in actual test conditions, the variation of kinematic (4.75 mm dia) and strain (2.38 mm dia) marker positions were determined for four-sets of three-second passive recordings taken at a 30° camera angle during biomechanical testing of a human medial collateral ligament (MCL) (Figure 2).

Complete details of this test configuration and marker placement can be found in our previous publications [4,14].

Accuracy of Simulated Strain Measurement. Accuracy tests were performed dynamically to determine the ability of the system to measure simulated 3D changes in strain. The effects of strain magnitude and camera angle were assessed. A 2.38 mm dia. marker was adhered to a fixed location, while a similar marker was adhered 13.5 mm apart ($L_{initial}$) to a linear actuator (Tol-O-Matic, Inc, Hamel, MN, accuracy ±0.0025 mm). The $L_{initial}$ was chosen to replicate the spacing between markers used to calculate 3D strains in the human MCL [4,14]. In two separate tests, the actuator was translated (ΔL) along either the z- or x-axis in Figure 1 to simulate strains of 1, 2, 5 and 20%. Tests were performed four times for each displacement. Accuracy was calculated as the difference between the predicted displacement and the known actuator displacement. The error in simulated strain measurement was computed by determining the absolute difference between actuator strain and DMAS strain ($\Delta L/L_{initial}$).

Accuracy of Kinematic Measurements. When tracking joint kinematics, it is desirable to establish "embedded" coordinate systems within the bones using a convention such as the one described by Grood and Suntay [16]. The transformation matrix between embedded coordinate systems is established by tracking markers on the bones that define separate "marker" coordinate systems. The transformation between one marker coordinate system and the corresponding embedded coordinate system on a bone does not change during testing. By establishing these transformations before testing and then tracking the transformation between marker coordinate systems during testing, the transformation between embedded coordinate systems can be determined [4,14]. To assess kinematic measurement accuracy, the setup and calculations necessary to record knee joint kinematics were simulated. Two L-shaped white blocks (the "kinematic blocks", Figure 2) with three 4.75 mm dia. black markers that formed a 90 degree angle were used to establish marker coordinate systems. The following tests were repeated four times for each translation or rotation, at camera angles of 30, 60 and 90 degrees.

To measure accuracy of translations along the z-axis in Figure 1 from kinematic calculations, one kinematic block was adhered to a static fixture and a second one was attached to the linear actuator. An Inscribe 3D Digitizer (Immersion Corp, San Jose, CA accuracy ±0.085 mm) was used to determine the centroids of the markers by digitizing points on the marker surface and then fitting the coordinates to the equation of a sphere. To simulate the use of embedded coordinate systems, three points on both the static fixture and the actuator were digitized and used to establish orthonormal coordinate systems. The transformation matrices were calculated between the kinematic blocks and their respective embedded coordinate systems. The actuator was displaced 0.500, 1.000, 5.000 and 50.000 mm and an overall transformation matrix between the embedded systems was calculated by concatenation. The ratio of the calculated translations to the known translations was computed.

To measure accuracy of translation measurements along the x-axis in Figure 1 from kinematic calculations, a kinematic block was adhered to an x-y table and the table was moved 0.50, 1.00, 5.00, and 50.00 mm, measured with digital calipers (Mitutoyo, San Jose, accuracy ±0.02 mm). Error was calculated as the ratio of translation predicted from the motion analysis data to the known translation.

To determine accuracy of rotations about the z-axis in Figure 1, a rotational actuator (Tol-O-Matic, Inc, Hamel, MN, accuracy ±0.002°) was used to rotate one of the kinematic blocks through angles of 2.00° and 20.00°. The transformation matrix between the two embedded coordinate systems was calculated and the rotation between the two systems was resolved using the method of Grood and Suntay [16]. The ratio of the rotation angle from the motion analysis data to the known angle was determined.

Statistical Analysis. The effects of camera angle and marker size on 3D precision were assessed using a two-way ANOVA with repeated measures. The effects of camera angle and strain magnitudes on x-axis and z-axis strain accuracy were assessed using two separate two-way ANOVAs with repeated measures. The effects of camera angle on x-axis and z-axis translational kinematic accuracy and z-axis rotational kinematic accuracy were assessed using two separate two-way ANOVAs with repeated measures. Statistical significance was set at $p<0.05$ for all analyses.

RESULTS

Precision. Results for precision were excellent for both marker sizes (Table 1). The larger markers exhibited significantly better precision than the smaller markers ($p=0.005$). There was no effect of camera angle on marker precision ($p=0.089$). The best results (±0.004 mm, 0.0020 % FOV) were obtained for the larger markers using a 30-degree camera angle. Precision did not vary considerably between the x, y and z coordinates of the markers. For example, at a 60 degree camera angle, the larger markers had x, y and z coordinate precisions of 0.019, 0.019 and 0.012 mm, respectively. The precisions for both marker sizes obtained with a MCL biomechanical test setup were comparable to precisions for the controlled tests (Table 1, 4th row of data).

Accuracy of Simulated Strain Measurement. The optical system delivered excellent results for strain error (Table 2). There was a significant effect of camera angle on accuracy for z- and x-axis strain accuracy ($p=0.004$ and $p<0.001$, respectively, Figure 3). The most accurate camera angle for strains along the z-axis was 30°, having an average accuracy of ±0.005 mm with a strain error of ±0.035%. Conversely, the most accurate camera angle when strains were measured along the x-axis was 90°, having average accuracies of ±0.003 resulting in a strain error of ±0.025%. There was a significant effect of strain magnitude on accuracy for z- and x-axis strain accuracy ($p=0.008$ and $p<0.001$, respectively). The condition conferring the least accuracy occurred for both the z-axis and x-axis cases at 90° and 30°, respectively, when a 20% strain was applied.

Accuracy of Kinematic Measurements. The optical system delivered very good results for kinematic accuracy (Table 3). Data for z-axis kinematic accuracy are shown as an example (Figure 4). The average x- and z-axis translational accuracies across all three camera angles and all four actuator displacements were ±0.025 and ±0.016 mm, respectively. Average accuracy for rotation was ±0.124° (Table 3). There was a significant effect of camera angle on accuracy of kinematic measurements of translation along the z- and x-axes ($p=0.029$ and $p<0.001$, respectively), but there was no effect of camera angle on kinematic rotational accuracy ($p=0.378$). The effect of camera angle on the kinematic translational accuracies was similar to that for the strain accuracies. There was a significant effect of the magnitude of translation/rotation on accuracy of kinematic measurements of translation along the z- and x-axes and rotation about the z-axis ($p<0.001$, $p<0.001$ and $p=0.033$, respectively). Larger translations/rotations reduced kinematic accuracy.

DISCUSSION

This study demonstrated that the 3D system can accurately measure simulated strain and kinematics using physical and optical conditions that accommodate simultaneous tracking of markers for both measurements. A reduced camera angle significantly improved accuracy for frontal plane (z-axis) displacements, while an increased camera angle significantly improved accuracies of displacements along the intersection of the saggital and transverse planes (x-axis). Moreover, in comparison to similar systems using proprietary vendor-specific hardware, this system is a small fraction of the cost.

Accuracy and precision of the system were determined using a testing environment that was specifically designed to mimic the physical and optical conditions for experiments on the human MCL in intact knees. For actual testing of the human MCL, only precision was determined. It is not possible to determine strain accuracy during an actual biomechanical test since a gold standard for strain measurements is difficult if not impossible to establish. However, by setting all testing variables (i.e., FOV, marker size, marker spacing, lighting) appropriately, the controlled tests faithfully reproduced the physical and optical conditions of actual biomechanical tests for the MCL. Results for precision from the controlled tests and from actual measurements on the MCL were similar (Table 1), supporting the notion that the controlled tests provided a good surrogate for the physical and optical conditions that are encountered during actual tests on the MCL.

System precision (Table 1) was calculated using the length of the position vectors of the markers, and thus these measurements should be considered average errors that take into account the precision in all three spatial directions. For the simulated strain measurements, the major spatial directions were accounted for by testing along the x- and z-axes. By positioning the cameras at an angle that permitted the most marker motion perpendicular to the cameras, therefore reducing the incremental distances that each pixel in the video system represents, the strain error was significantly decreased. For z-axis strains this occurred at a 30° camera angle, and for x-axis strains this occurred at a 90° camera angle. Based upon the accuracy results (Figure 3), it is recommended that these camera angles be optimized accordingly, especially if large strains are predicted. The measurements of strain accuracy should be considered a best case when considering general measurements in 3D using comparable camera angles. Although a similar argument applies to the kinematic measurements, the "gold standard" for these measurements was based on a combination of digitizer, actuator encoder, or digital caliper measurements. Because of differences in the accuracy of these measurement techniques and the propagation of errors in the kinematic measurements, the results for translational and rotational kinematic accuracies likely represent worst cases. This error propagation is likely responsible for the reduction of accuracy with increased axial translation (Figure 4).

As with any system based on video or digital cameras, the most important determinants of precision and accuracy are the resolution of the CCD and the FOV used for measurements. This assumes that an accurate DLT calibration has been performed and that this calibration has taken into account errors associated with lens distortion. In this study, the FOV was chosen to allow simultaneous tracking of markers for strain and kinematic measurements in the context of studying the human MCL [4,14]. Limitations on the rate of data transfer from the camera to the framegrabber cards and then to computer memory, primarily imposed by the bandwidth of the computer system's bus, result in a tradeoff between the frame rate and spatial resolution of the CCD. Cameras with higher resolution CCDs typically have slower frame rates. This limitation will likely be eliminated with improvements in computer architecture. Marker contrast is also very important, with improved contrast yielding better system precision and thus accuracy. During actual biomechanical testing, contrast may become reduced by extraneous objects in the foreground and background. Draping the testing backdrop and fixtures with white material, and applying white gauze to any uninvolved tissue that may darken the captured image will alleviate this problem. Extreme specimen discoloration could similarly reduce marker contrast. Affixing the strain markers to the tissue with adhesives may cause local strain abnormalities; therefore a minimal amount of adhesive should be applied. Finally, the physical size of a CCD affects the sensitivity through its responsivity and dynamic range, with larger CCDs yielding better sensitivity and thus better image quality (see, e.g., [17]). The cameras used in this study had 1” CCDs, the largest size that was available.

In summary, the 3D measurement system provided excellent accuracy for simulated strain measurement and very good accuracy for kinematic measurements. The absolute and percent errors are considered to be more than acceptable for simultaneous 3D measurements of ligament strain and joint kinematics.

ACKNOWLEDGMENTS

Financial support from NIH grant #AR47369 is gratefully acknowledged.

REFERENCES

[1] Mazzocca, A. D., Nissen, C. W., Geary, M., and Adams, D. J., 2003, "Valgus Medial Collateral Ligament Rupture Causes Concomitant Loading and Damage of the Anterior Cruciate Ligament," J Knee Surg, **16**, pp. 148-51.

[2] Hull, M. L., Berns, G. S., Varma, H., and Patterson, H. A., 1996, "Strain in the Medial Collateral Ligament of the Human Knee under Single and Combined Loads," J Biomech, **29**, pp. 199-206.

[3] Saeki, K., Mihalko, W. M., Patel, V., Conway, J., Naito, M., Thrum, H., Vandenneuker, H., and Whiteside, L. A., 2001, "Stability after Medial Collateral Ligament Release in Total Knee Arthroplasty," Clin Orthop, pp. 184-9.

[4] Gardiner, J. C. and Weiss, J. A., 2003, "Subject-Specific Finite Element Analysis of the Human Medial Collateral Ligament During Valgus Knee Loading," J Orthop Res, **21**, pp. 1098-106.

[5] Kuo, L. C., Su, F. C., Chiu, H. Y., and Yu, C. Y., 2002, "Feasibility of Using a Video-Based Motion Analysis System for Measuring Thumb Kinematics," J Biomech, **35**, pp. 1499-506.

[6] An, K. N., Growney, E., and Chao, E. Y., 1991, "Measurement of Joint Kinematics Using Expertvision System," Biomed Sci Instrum, **27**, pp. 245-52.

[7] Kovaleski, J. E., Hollis, J., Heitman, R. J., Gurchiek, L. R., and Pearsall, A. W. t., 2002, "Assessment of Ankle-Subtalar-Joint-Complex Laxity Using an Instrumented Ankle Arthrometer: An Experimental Cadaveric Investigation," J Athl Train, **37**, pp. 467-474.

[8] Kirstukas, S. J., Lewis, J. L., and Erdman, A. G., 1992, "6r Instrumented Spatial Linkages for Anatomical Joint Motion Measurement--Part 2: Calibration," J Biomech Eng, **114**, pp. 101-10.

[9] Hefzy, M. S., Ebraheim, N., Mekhail, A., Caruntu, D., Lin, H., and Yeasting, R., 2003, "Kinematics of the Human Pelvis Following Open Book Injury," Med Eng Phys, **25**, pp. 259-74.

[10] Ezzet, K. A., Hershey, A. L., D'Lima, D. D., Irby, S. E., Kaufman, K. R., and Colwell, C. W., Jr., 2001, "Patellar Tracking in Total Knee Arthroplasty: Inset Versus Onset Design," J Arthroplasty, **16**, pp. 838-43.

[11] Meskers, C. G., Fraterman, H., van der Helm, F. C., Vermeulen, H. M., and Rozing, P. M., 1999, "Calibration of the "Flock of Birds" Electromagnetic Tracking Device and Its Application in Shoulder Motion Studies," J Biomech, **32**, pp. 629-33.

[12] Cerulli, G., Benoit, D. L., Lamontagne, M., Caraffa, A., and Liti, A., 2003, "In Vivo Anterior Cruciate Ligament Strain Behaviour During a Rapid Deceleration Movement: Case Report," Knee Surg Sports Traumatol Arthrosc, **11**, pp. 307-11.

[13] Fleming, B. C. and Beynnon, B. D., 2004, "In Vivo Measurement of Ligament/Tendon Strains and Forces: A Review," Ann Biomed Eng, **32**, pp. 318-28.

[14] Gardiner, J. C., Weiss, J. A., and Rosenberg, T. D., 2001, "Strain in the Human Medial Collateral Ligament During Valgus Loading of the Knee," Clin Orthop, pp. 266-74.

[15] Hatze, H., 1988, "High-Precision Three-Dimensional Photogrammetric Calibration and Object Space Reconstruction Using a Modified Dlt-Approach," J Biomech, **21**, pp. 533-8.

[16] Grood, E. S. and Suntay, W. J., 1983, "A Joint Coordinate System for the Clinical Description of Three-Dimensional Motions: Application to the Knee," J Biomech Eng, **105**, pp. 136-44.

[17] Anonymous, "Ccd Performance and the Pixel Size (Chip Size)," TH-1084, 1998.

	4.75 mm dia. Markers		2.38 mm dia. Markers	
Camera Angle (θ)	Precision (mm)	Percent FOV (%)	Precision (mm)	Percent FOV (%)
30°	0.004	0.0020%	0.035	0.0163%
60°	0.011	0.0049%	0.025	0.0117%
90°	0.006	0.0026%	0.012	0.0048%
MCL Study (30°)	.009	0.0044%	0.011	0.0054%

<u>Table 1:</u> Results for measurement of 3D precision. The first three rows of data were obtained by recording stationary markers for 25 seconds with a FOV of 190 mm. The fourth row was obtained from passive recording acquired during biomechanical testing of a human MCL. Each passive recording was approximately 3 seconds long, with a camera angle of 30°, and a FOV of 190 mm. Absolute precision was calculated as two standard deviations of the position measurement, while Percent FOV was calculated as the precision divided by the FOV multiplied by 100.

	Camera Angle (θ)		**1.0% Strain**	**2.0% Strain**	**5.0% Strain**	**20.0% Strain**	**Averages across all Strains**
z-axis	30°	Accuracy (mm)	0.004 ± 0.007	0.011 ± 0.003	0.003 ± 0.004	0.001 ± 0.007	**0.005 ± 0.005**
		Strain Error (%)	0.028 ± 0.052	0.084 ± 0.018	0.019 ± 0.030	0.010 ± 0.052	0.035 ± 0.033
	60°	Accuracy (mm)	0.002 ± 0.001	0.013 ± 0.005	0.005 ± 0.005	0.009 ± 0.012	**0.007 ± 0.006**
		Strain Error (%)	0.014 ± 0.009	0.099 ± 0.037	0.040 ± 0.035	0.067 ± 0.091	0.055 ± 0.037
	90°	Accuracy (mm)	0.009 ± 0.001	0.016 ± 0.003	0.011 ± 0.004	0.024 ± 0.005	**0.015 ± 0.003**
		Strain Error (%)	0.065 ± 0.006	0.115 ± 0.025	0.081 ± 0.027	0.175 ± 0.034	0.109 ± 0.049
x-axis	30°	Accuracy (mm)	0.011 ± 0.002	0.011 ± 0.002	0.019 ± 0.002	0.036 ± 0.003	**0.019 ± 0.012**
		Strain Error (%)	0.081 ± 0.018	0.082 ± 0.014	0.138 ± 0.017	0.267 ± 0.024	0.142 ± 0.088
	60°	Accuracy (mm)	0.002 ± 0.002	0.018 ± 0.002	0.006 ± 0.011	0.003 ± 0.002	**0.007 ± 0.007**
		Strain Error (%)	0.015 ± 0.015	0.130 ± 0.017	0.045 ± 0.082	0.021 ± 0.011	0.053 ± 0.053
	90°	Accuracy (mm)	0.002 ± 0.001	0.006 ± 0.001	0.003 ± 0.007	0.003 ± 0.001	**0.003 ± 0.002**
		Strain Error (%)	0.017 ± 0.008	0.045 ± 0.007	0.022 ± 0.049	0.018 ± 0.006	0.025 ± 0.013

<u>Table 2:</u> Accuracy of 3D simulated strain measurement along the z- and x-axes for all four strain levels. Accuracy (mm) was calculated as the difference between the actuator-based value and the value calculated from the optical system data. Strain error (%) is the accuracy divided by the gauge length (13.5 mm) multiplied by 100.

	Translation (x-axis)		Translation (z-axis)		Rotation (z-axis)	
Camera Angle (θ)	Accuracy (mm)	% FOV	Accuracy (mm)	% FOV	Accuracy (deg)	% FOV
30°	0.034 ± 0.031	0.012 ± 0.004%	0.008 ± 0.011	0.005 ± 0.006%	0.132 ± 0.162	0.074 ± 0.091%
60°	0.018 ± 0.005	0.009 ± 0.006%	0.019 ± 0.023	0.009 ± 0.010%	0.082 ± 0.069	0.043 ± 0.036%
90°	0.021 ± 0.002	0.009 ± 0.008%	0.020 ± 0.017	0.006 ± 0.005%	0.160 ± 0.218	0.074 ± 0.101%

Table 3: Accuracy of 3D kinematic measurements. Accuracy is the difference between the actuator translation/rotation and the value calculated from the optical system data. Accuracy in terms of Percent FOV is the accuracy divided by FOV multiplied by 100. Results are the average across all translations/rotations descibed in the Methods section.

FIGURE CAPTIONS

Figure 1: Plan view of the camera setup. The z-axis is directed out of the page. To assess system sensitivity to camera angle, angles of 30, 60 and 90 degrees were used during testing.

Figure 2: Photograph of test setup for simultaneous measurement of MCL strain and knee joint kinematics. Eighteen markers (2.38 mm dia) were adhered to the MCL for strain measurement. Femoral and tibial kinematic blocks, each with three kinematic markers (4.75 mm dia), were affixed to the cortical bone.

Figure 3: Results for determination of simulated 3D strain along the z- and x-axes. Strain Error was computed as the difference between the actuator-based strain and the strain calculated by the motion analysis system, divided by the gauge length.

Figure 4: Results for the measurement of 3D kinematics along the z-axis direction. Accuracy was measured as the difference between the actuator based translation and the value calculated by the motion analysis system, divided by the actuator translation.

Figure 1

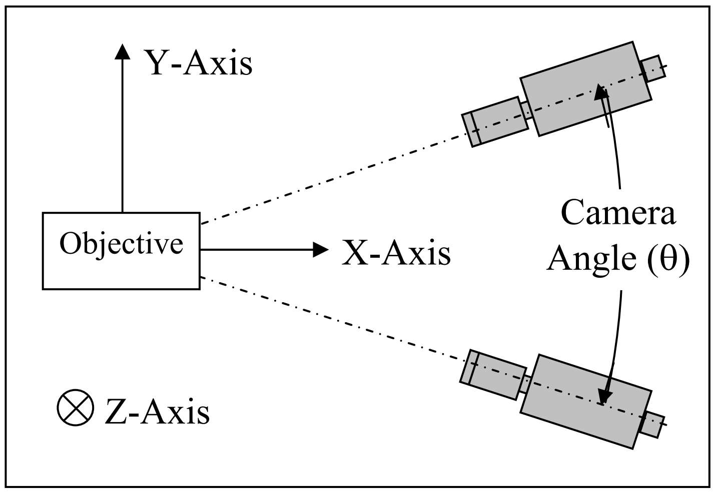

Figure 2

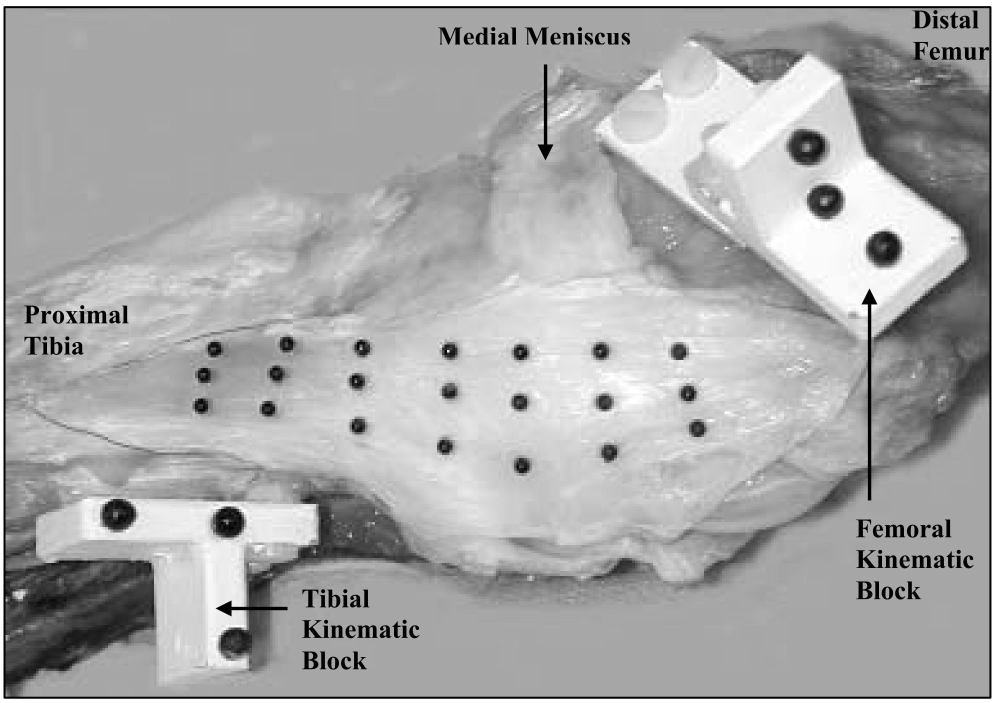
Medial Meniscus
Distal Femur
Proximal Tibia
Femoral Kinematic Block
Tibial Kinematic Block

Figure 3

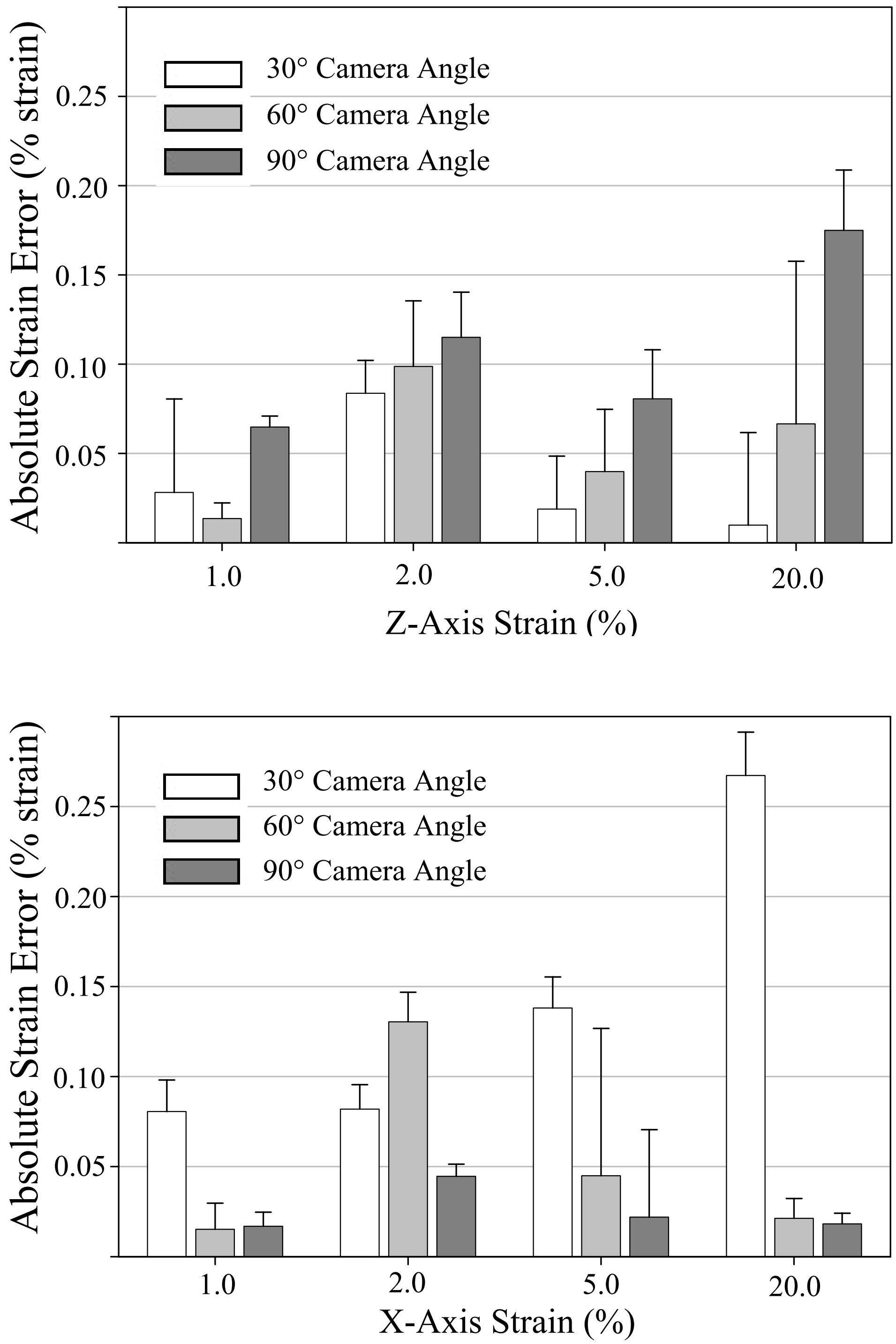
30° Camera Angle
60° Camera Angle
90° Camera Angle
Absolute Strain Error (% strain)
0.25
0.20
0.15
0.10
0.05
1.0
2.0
5.0
20.0
Z-Axis Strain (%)
30° Camera Angle
60° Camera Angle
90° Camera Angle
Absolute Strain Error (% strain)
0.25
0.20
0.15
0.10
0.05
1.0
2.0
5.0
20.0
X-Axis Strain (%)

Figure 4

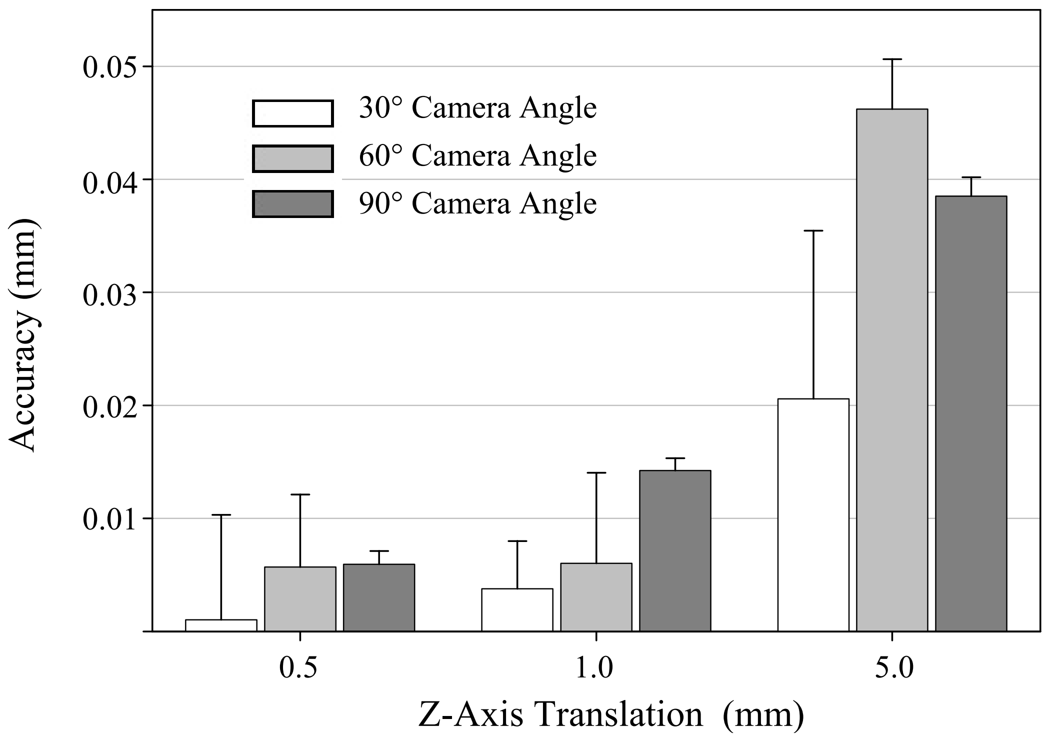
0.05
0.04
0.03
0.02
0.01
Accuracy (mm)
30° Camera Angle
60° Camera Angle
90° Camera Angle
0.5
1.0
5.0
Z-Axis Translation (mm)